

ARTICLE

Highly sensitive quartz crystal microbalance sensor modified with antifouling microgels for saliva glucose monitoring

Received 00th January 20xx,
Accepted 00th January 20xx

DOI: 10.1039/x0xx00000x

Qian Dou,^{a,b} Shiwen Wang,^b Zifeng Zhang,^{a,b} Yanxiang Wang,^e Zhipeng Zhao,^b Haijian Guo,^f Hongliang Liu^{*d} and Qing Dai^{*,a,b,c}

Saliva glucose detection based on quartz crystal microbalance (QCM) technology has become an important research direction of non-invasive blood glucose monitoring. However, the performance of this label-free glucose sensors are heavily deteriorated by the large amount of protein contaminants in saliva. Here, we successfully achieved the direct detection of saliva glucose by endowing the microgels on the QCM chip with superior protein-resistive and glucose-sensitive properties. Specifically, the microgel networks provide plenty of boric acid binding sites to amplify the signals of targeted glucose. The amino acid layer wrapped around the microgel and crosslinking layer can effectively eliminate the impact of non-specific proteins in saliva. The designed QCM sensor has a good linearity in the glucose concentration range of 0–40 mg/L at pH 6.8–7.5, satisfying the physiological conditions of saliva glucose. Moreover, the sensor has excellent ability to tolerate proteins, enabling it to detect glucose in 50% human saliva. This result provides a new approach for non-invasive blood glucose monitoring based on QCM.

Introduction

Diabetes mellitus is a worldwide public health problem and the diagnosis and treatment of diabetes require a regular or, ideally, continuous detection of glucose levels in blood.^{1–5} The blood glucose level can now be measured by following two mainstream methods: one is finger blood or venous blood, and the other is to insert a micro probe into the skin to continuously measure glucose in the intercellular fluid. However, neither of these invasive detection has enough patient compliance for daily use.^{6,7} Therefore, non-invasive technique for glucose detection has become a research hotspot in diabetes in the past thirty years.^{8,9} Recently, monitoring glucose in body fluid, such as urine, sweat, tears and saliva has been investigated intensively to realize blood glucose monitoring.^{10,11} Especially, saliva has attracted more and more attention, not only due to the high correlation between saliva glucose concentrations and

blood glucose levels but also the intrinsic advantages of saliva, including its safety and convenience of real-time collection.^{12,13}

The concentration of glucose in saliva is approximately 1/100–1/50 (3.6–36 mg/L)¹⁴ that of blood sugar. Therefore instrument with higher sensitivity—quartz crystal microbalance (QCM) has been developed for detecting the saliva glucose, which has become successful for the on-line detection of nucleic acids, proteins, bacteria, and many other molecular recognition

events in the liquid form because of its low-cost, label-free and real-time measurement capability.^{15–25} However, the highly non-specific interaction with the sensor interface caused by proteins in saliva (the total amount of protein in saliva can reach thousands of milligrams per liter)^{26,27} makes it difficult to recognize small frequency changes generated by the binding of glucose molecules with their receptors on the surface from the total frequency response (Figure S1 in the Supporting Information).^{28–31}

In our previous work, we have successfully implemented boric acid hydrogel combined with QCM to detect saliva glucose in phosphate buffer solution (PBS) and artificial saliva under physiological conditions. However, the non-specific adsorption of a large number of proteins resulted in inaccurate results in human saliva detection. Herein, we synthesized a film on the QCM chip to overcome the non-specific adsorption of proteins while detecting saliva glucose. Specifically, microgels containing boric acid segments were used as multi-binding sites for glucose. ³²Amino acids grafted onto the microgels were used as protein-resistive component, and were subsequently fixed on the chip by chemical crosslinking. The designed glucose sensor exhibits

^a School of Materials Science and Engineering, Zhengzhou University, Zhengzhou 450001, P. R. China.

^b Division of Nanophotonics, CAS key laboratory of Standardization and Measurement for Nanotechnology, CAS Center for Excellence in Nanoscience, National Center for Nanoscience and Technology, Beijing 100190, P. R. China.

^c Center of Materials School and Optoelectronics, University of Chinese Academy of Sciences, Beijing 100049, P. R. China.

^d CAS Key Laboratory of Bio-Inspired Materials and Interfacial Science, Technical Institute of Physics and Chemistry, Chinese Academy of Sciences, Beijing 100190, P. R. China.

^e Institute of Medicinal Biotechnology, Chinese Academy of Medical Sciences and Peking Union Medical College, Beijing 100050, China.

^f Jiangsu Provincial Center for Disease Control and Prevention, Nanjing 210009, P. R. China.

Electronic Supplementary Information (ESI) available: [details of any supplementary information available should be included here]. See DOI: 10.1039/x0xx00000x

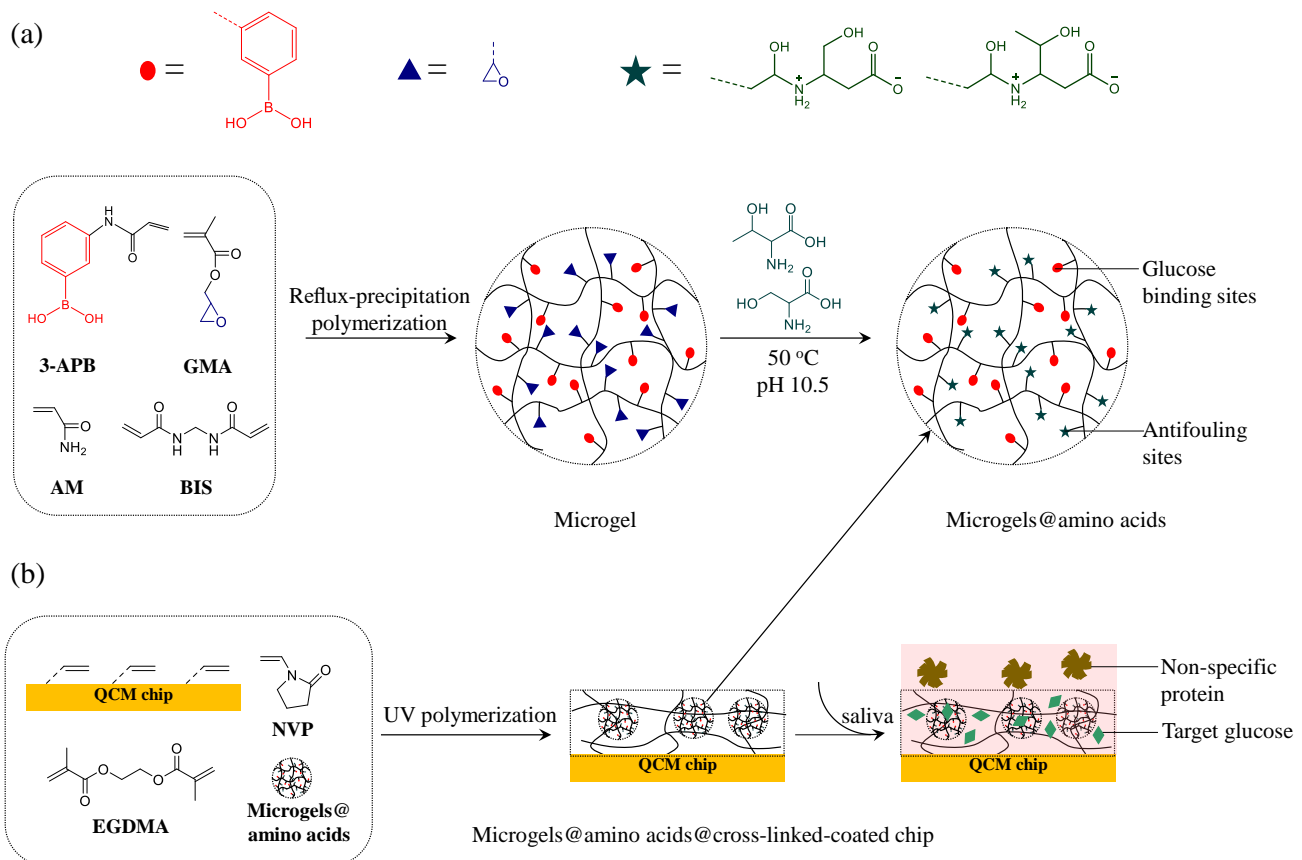


Fig. 1(a) Synthesis of microgels through reflux-precipitation polymerization and amino acids grafting onto the surface of microgels by a ‘click reaction’. **(b)** The microgels@amino acids were immobilized on the QCM chip by chemical crosslinking.

glucose-responsive and pollutant-resistant properties. The sensor can detect saliva glucose at 0–40 mg/L under physiological conditions and possesses the superior ability of tolerating proteins and organic molecules, achieving the detection of glucose in 50% human saliva.

Results and discussion

The polymer-coated chip was synthesized in three steps. Boric acid microgels have high glucose sensitivity and chemical stability^{33,34} and were obtained by reflux-precipitation polymerization (Figure 1a).³⁵ Neutral amino acids (threonine and serine with a molar ratio of 1:1) were then grafted onto the microgels by a ‘click reaction’,³⁶ which has attracted increasing attention due to its zwitterionic, biomimetic nature, convenient source, good chemical stability and excellent anti-biological pollution performance.^{37,38} The microgels were covered by a zwitterionic surface with a protonated secondary amine cation (-NH_2^+) and deprotonated carboxyl anion (-COO^-). Because the inside of microgels had epoxy groups, which had amino acids after the “click reaction”. The amino acid layer was able to bind a significant amount of water molecules due to the formation of a hydration layer via electrostatic interactions and hydrogen bonding, which led to a strong protein repulsive force at specific separations.^{39,40} Finally, chemical crosslinking was used to fix

the microgels@amino acids onto the double-bonded⁴¹ QCM chip (Figure 1b). Thus, core–shell microgels@amino acids with a glucose-sensitive core and protein-tolerant shell were obtained (Figure S2 in the Supporting Information).⁴² When saliva was added to the polymer-coated chip, glucose molecules were recognized while resisting the non-specific adsorption of proteins.

In each step of the synthesis process, the roles of the compounds involved are summarized. 3-(acrylamido) phenylboronic acid (3-APB), glycidyl methacrylate (GMA), acrylamide (AM) and N,N'-methylenebisacrylamide (BIS) are used to synthesize microgels. 3-APB contains boric acid groups that is used to recognize glucose. GMA contains epoxy groups that is used to graft amino acids. AM contains amino groups and is used as hydrophilic material. BIS contains double bonds at both ends and is used as a cross-linking agent. N-vinylpyrrolidone (NVP) and ethyleneglycoldimethacrylate (EGDMA) are used to synthesize crosslinking layer on QCM chip (The crosslinking mechanism is shown in Figure S3 in the Supporting Information). NVP is used as polymerization monomer, because polyvinylpyrrolidone (PVP) has anti-protein function, good chemical stability and film formation.^{43,44} EGDMA contains double bonds and is used as crosslinking agent.

FTIR spectrum of the synthetic products are shown in Figure 2a. The microgels revealed two peaks at $\sim 3303 \text{ cm}^{-1}$ and

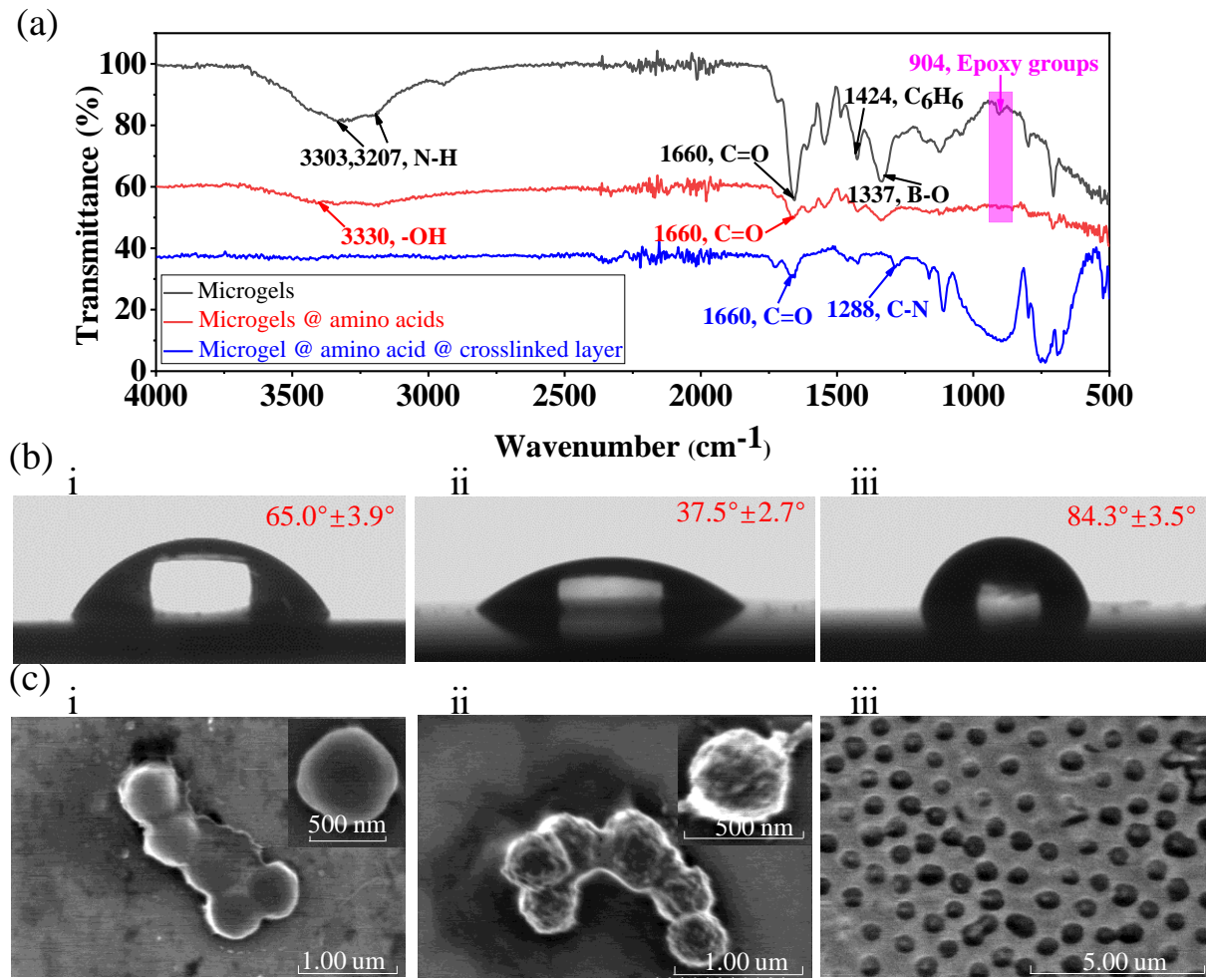


Fig. 2(a) FTIR spectrum of the synthetic products. (b) Water contact angles of microgels (i), microgels@amino acids (ii), and microgels@amino acids@crosslinked layer (iii). The data indicate the s.d. of three replicating measurements. (c) Microgels had a smooth surface, uniform size, and spherical morphology (i), while the surface of microgels@amino acids was uneven (ii). The microgels@amino acids were wrapped in the crosslinked layer (iii).

~3207 cm⁻¹ corresponding to the vibration absorption peaks of N-H as well as a strong C=O stretch vibration peak at ~1660 cm⁻¹. At lower wavenumbers, the characteristic absorption peaks of benzene ring appeared at ~1424 cm⁻¹ and an adsorption peak at ~1337 cm⁻¹ was attributed to B-O. Finally, the peak at ~904 cm⁻¹ was a characteristic of epoxy groups.³⁶ These results confirmed the formation of boric acid microgels. Furthermore, the peak at ~3330 cm⁻¹ was attributed to the vibration absorption of -OH. Following the grafting of amino acids onto the surface of microgels, the characteristic peak of the epoxy groups (~904 cm⁻¹) disappeared. Finally, the peak at ~1662 cm⁻¹ and ~1288 cm⁻¹ were attributed to the stretching vibration of C=O and C-N (displayed in blue), demonstrating the formation of crosslinked layers.

The hydrophilicity of the products were assessed using contact angle measurements. Microgels and microgel@amino acids were evenly dispersed in ethanol and coated on the chip with a spin coater. The water contact angle of microgel@amino acids was 37.5°±2.7° (Figure 2b- ii), approximately half of the

water contact angle of pure microgels (65.0°±3.9°, Figure 2b- i). This increase in hydrophilicity is beneficial in the shielding of proteins. Further, the water contact angle of the crosslinked layer was 84.3°±3.5° (Figure 2b-iii).

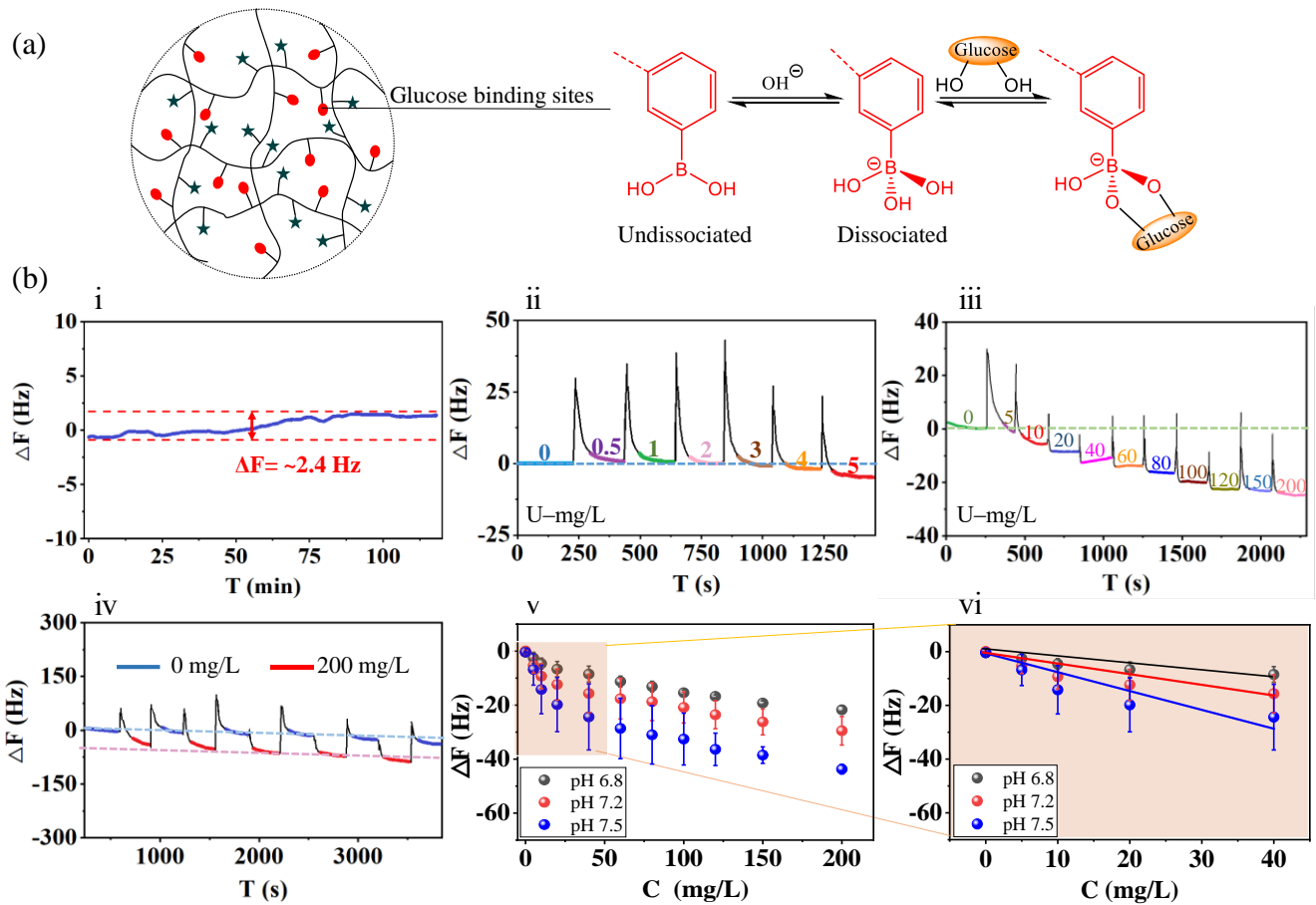


Fig. 3(a) The binding mechanism between PBA and glucose. **(b- i)** The sensor has good stability and the ΔF was only $\sim 2.4 \text{ Hz}$ within almost 2 h. **(b- ii)** The detection limit of the glucose sensor was 5 mg/L. **(b- iii)** The glucose sensor had a good response to different concentrations of glucose. **(b-iv)** Binding of glucose was reversible. **(b- v)** The ΔF became more negative with the increase in pH. Error bars indicate the s.d. of three replicating measurements. **(b- vi)** Favorable linear relationship between ΔF and different glucose concentrations from 0 to 40 mg/L at different pH values. Error bars indicate the s.d. of three replicating measurements.

Scanning electron microscopy was used to evaluate the morphology and particle size of the materials. The microgels had a smooth surface, uniform size ($\sim 600 \text{ nm}$), and spherical morphology (Figure 2c- i). Following amino acid grafted onto the surface of the microgels, the surface appeared uneven (Figure 2c- ii), and many of the pellets (microgels@amino acids) were wrapped within the crosslinked layer (Figure 2c- iii), further proving that the microgel@amino acids were successfully fixed onto the QCM chip.

Phenylboronic acid (PBA) exists in two forms in aqueous solution, namely in a negatively charged dissociated state and in an uncharged non-dissociated state. A dissociation equilibrium exists between these two states. Non-dissociated PBA is a flat triangle and forms an unstable complex with glucose, while dissociated PBA has a tetrahedral structure and can form cyclic lactones with glucose (Figure 3a).⁴⁵⁻⁴⁷

The feasibility of a glucose sensor to monitor changes in glucose concentrations was evaluated in PBS. The frequency shift (ΔF) is equal to the frequency of the glucose sample minus the frequency of the blank sample. Firstly, the stability of the glucose sensor was evaluated in PBS, the fluctuation value of ΔF

was only $\sim 2.4 \text{ Hz}$ when the polymer-coated chip exposed to PBS for almost 2 h (Figure 3b- i). Subsequently, in order to obtain the detection limit of the glucose sensor, we gradually increased the glucose concentration. When the glucose concentration increased to 5 mg/L, ΔF had a relatively obvious decrease (Figure 3b- ii). So the detection limit of glucose sensor was 5 mg/L. Furthermore, an obvious decrease in resonance frequency was observed when the glucose concentrations increased from 0 mg/L to 200 mg/L (Figure 3b- iii).

One of the best advantages of the reaction between glucose and boronic acid is its reversibility, allowing the disruption of the network built on PBA–diol complex via adding glucose afterward.⁴⁸ As illustrated in Figure 3b- iv , the sensor response, furtherly, to multiple alternating exposures to 200 mg/L glucose and 0 mg/L glucose in PBS solution was constant.

The shift in resonance frequency was plotted as a function of glucose concentration under different pH conditions (Figure 3b- v). The ΔF became more negative with increasing pH at all three investigated pH conditions. Because higher pH facilitates the association of boronic acid molecules in the hydrogel network with glucose molecules. The sensor showed a good

linearity from 0 to 40 mg/L (Figure 3b- vi), adequately encompassing the range of glucose concentration in saliva under physiological conditions. The linear correlation coefficients were 0.9523 (pH 6.8), 0.9274 (pH 7.2), and 0.9482 (pH 7.5), respectively.

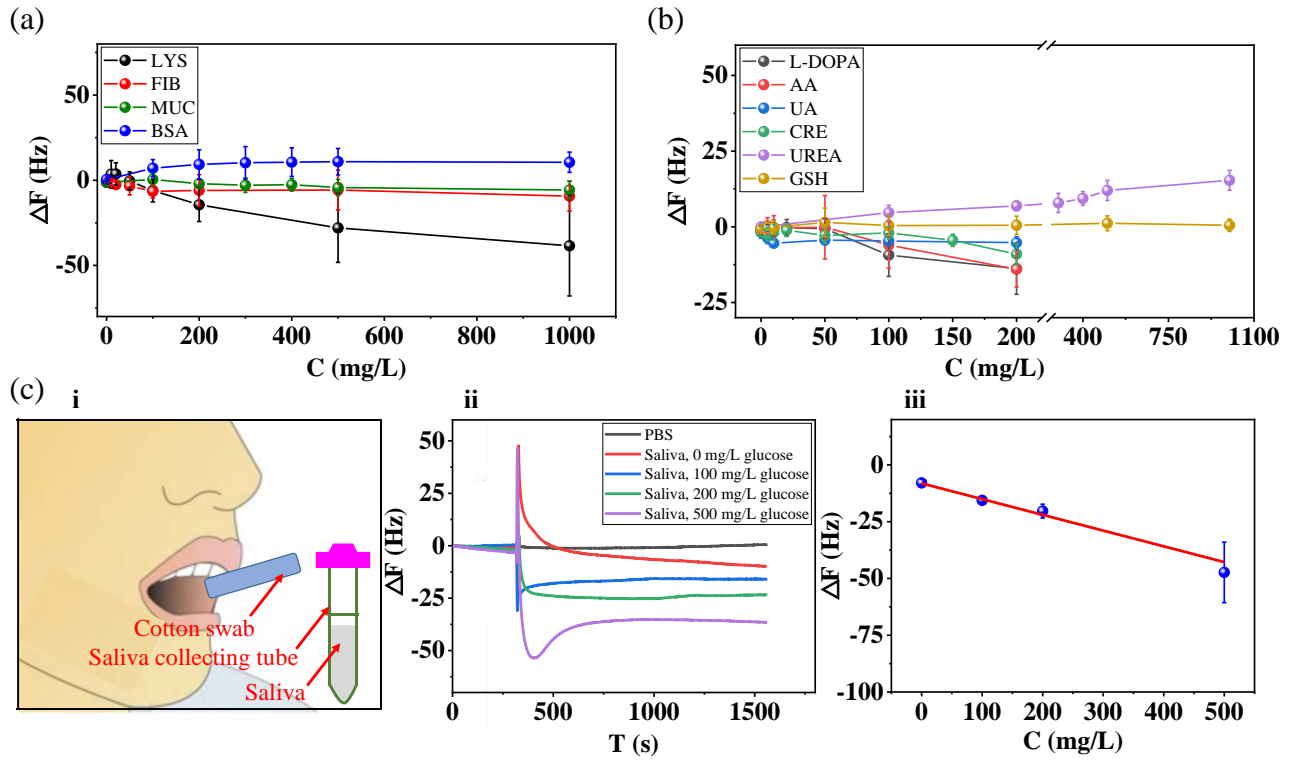


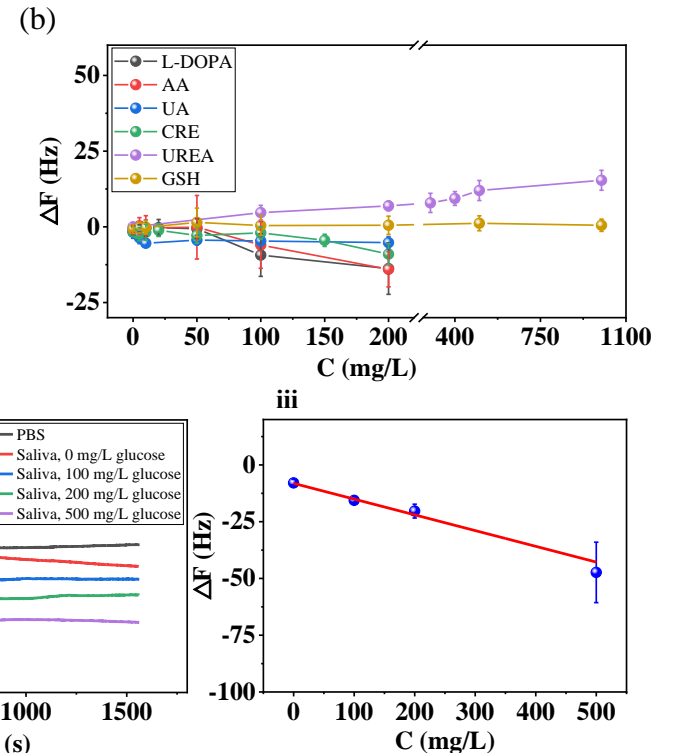
Fig. 4(a) Effects of proteins commonly found in saliva (BSA, MUC, FIB and LYS) on glucose sensors. Error bars indicate the s.d. of three replicating measurements. **(b)** Effects of common organics in saliva (GSH, UREA, CRE, UA, AA and L-DOPA) on glucose sensors. Error bars indicate the s.d. of three replicating measurements. **(c- i)** Using a saliva collection tube to collect saliva. **(c- ii)** As the glucose concentration increased, ΔF showed a downward trend in 50% human saliva. **(c- iii)** Good linear relationship between ΔF and glucose concentration. Error bars indicate the s.d. of three replicating measurements.

The resistance of the glucose sensor to common proteins in saliva, including bovine serum albumin (BSA), fibrinogen (FIB), mucin (MUC), and lysozyme (LYS), was verified in PBS solution.^{49,50} At a glucose concentration of 200 mg/L, the ΔF was -43.7 ± 1.8 Hz (Figure 3b- v), whereas, under the same test conditions, the concentration of BSA, FIB, and MUC were all 5-fold that of glucose (1000 mg/L), with quite small ΔF of 10.6 ± 5.9 Hz, -5.7 ± 5.2 Hz, and -9.3 ± 8.7 Hz, respectively (Figure 4a). When the concentration of LYS was 1000 mg/L, the ΔF was -38.5 ± 29.4 Hz (The microgels-coated sensors and microgels@crosslinked layer-coated sensor are used as comparative experiment, and the results are shown in Figure S4a, b, c, d and Table S1 in the Supporting Information). From the above results, the glucose sensor had excellent resistance to these four proteins. The superior anti-protein performance mainly benefits from the amino acid layer and crosslinking layer.

The glucose-detection interference by various common organic molecules in human saliva, e.g. urea, uric acid (UA), ascorbic acid (AA), levodopa (L-DOPA), l-glutathione (GSH) and creatinine (CRE), was also investigated.⁵⁰ GSH showed almost no interference at concentrations up to 1000 mg/L. The ΔF of

urea, CRE, UA, AA, and L-DOPA were minimal, at 6.9 ± 1.6 Hz, -1.1 ± 2.1 Hz, -5.2 ± 2.0 Hz, -14.0 ± 5.8 Hz, and -13.8 ± 8.5 Hz, respectively, at the same concentration as glucose (200 mg/L).

In order to further demonstrate the anti-pollution performance of the glucose sensor, human saliva was used to



detect glucose levels. A cotton swab was placed in the mouth and chewed for 2–3 minutes to fully absorb the saliva, then it was placed in a saliva collection tube and centrifuged to obtain saliva. An equal volume of saliva and PBS were mixed, and different amounts of glucose were added. As the glucose concentrations gradually increase, the ΔF became more negative (Figure 4c- ii). The glucose concentrations had a good linear relationship with the ΔF , with a linear correlation coefficient of 0.9671 (Figure 4c- iii).

Conclusions

We design a QCM glucose sensor with protein-resistive function to achieve the high-sensitivity detection of saliva glucose. Microgel containing boric acid segments are used as multi-binding sites for glucose, amino acid layer and crosslinking layer are used as the protein-resistive component. The experimental results show that the glucose sensor is compatible with physiological conditions and responses glucose range is from 0 to 40 mg/L. This designed sensor demonstrates great performance on reducing the nonspecific interference caused

by the proteins in saliva, which make it more practicable as a non-invasive glucose detection for daily-use.

Experimental section

Instruments. Glucose and anti-pollution tests were performed by using QCM 200 (SRS). The surface morphologies of materials were investigated using scanning electron microscope (S-4800). Hydrophilicity was measured by full automatic contact angle measuring instrument (Dsa-100) and the dispersant was ethanol. The functional groups of materials were determined by Microinfrared spectrometer (SP-200i). The surface morphologies of microgels were investigated by atomic force microscopy (M8-HR) in dry state and in aqueous solution. The forces applied during the preparation of crosslinked polymer films was realized by lab-built pressure film machine. Ultraviolet polymerization was achieved by UV lamp (The wavelength is 365 nm and the maximum power is 3 W). Saliva was collected through saliva collection tube (no disposal of cotton swabs) and were obtained through a centrifuge (AXTD4).

Reagents. Glycidyl methacrylate (GMA, 97%), N-vinyl-2-pyrrolidinone (NVP, 99%), acrylamide (AM, 98.5%) and ethylene glycol dimethacrylate (EGDMA, 98%) were purchased from Shanghai Macklin Biochemical Co., Ltd. 2,2-dimethoxy-1,2-diphenyl-ethanone (DMPA, >98%) and 2,2'-azobis(isobutyronitrile) (AIBN, >98%) were purchased from TCI (Shanghai) Development Co., Ltd. 3-aminopropyltriethoxysilane (APTES, 98%) was purchased from Alfa Aesar (China) Chemicals Co., Ltd. 3-(acrylamido) phenylboronic acid (3-APB, 98%) was purchased from Tianjin HeownsBiochem LLC. N,N'-methylenebisacrylamide (BIS, 98%) was purchased from Sinopharm Chemical Reagent Ltd. Dimethyl sulfoxide (DMSO), glucose, threonine, serine, sodium phosphate dibasic dodecahydrate, potassium dihydrogen phosphate, maleic anhydride, bovine serum albumin (BSA), lysozyme (LYS), fibrinogen (FIB), mucin (MUC), urea, uric acid (UA), ascorbic acid (AA), levodopa (L-DOPA), L-glutathione (GSH) and creatinine (CRE) are all pure analytical reagents.

Saliva experiment. Saliva collection was supported by the project "early identification, early diagnosis and cutting point of diabetes risk factors" (2016YFC1305700). The saliva samples were collected from ordinary urban and rural residents in Yancheng City, Jiangsu Province, China, and the age requirement was 18 to 65. People with mental disorders, pregnant and lactating women were not included. The standardized operation process of this project was performed complying with the medical ethics committee of Jiangsu Provincial Center for Disease Control and Prevention (JSJK2017-B003-02).

Saliva collection tubes were used to collect subjects' fasting saliva. Saliva collection tubes were centrifuged to obtain saliva (4000 r/min) without any additional treatment.

Surface modification of QCM chip. The QCM chip was sonicated for 10 min with piranha solution (H_2SO_4 (96% w/w) with H_2O_2 (30% w/w) in a volume ratio of 7:3). The processed chip was washed with redistilled water and dried with N_2 , then immersed

in a mixed solution of 3-aminopropyltriethoxysilane (100 μ L) and ethanol (50 mL) at room temperature. After 12 h, the QCM chip was rinsed with ethanol and subsequently dried with N_2 . The dried chip was immersed in a mixed solution of maleic anhydride (1 g) and N,N-dimethylformamide (50 mL) for 12 h. Finally, the treated chip was rinsed with ethanol and dried with N_2 .^{51,52}

Preparation of microgels. 3-APB (516 mg), AM (831 mg), GMA (350 μ L), BIS (46.2 mg), and AIBN (5 mg) were added to 40 mL of acetonitrile and refluxed at 90 $^{\circ}$ C for 1 h. After centrifugation, microgels were obtained and washed repeatedly with distilled water.³⁵

Preparation of microgels@amino acids. Threonine (119.1 mg) and serine (105.1 mg) were sonically dispersed in 50 mL of ethanol solution ($V_{ethanol}$: V_{water} = 1:3) and the pH value was adjusted to 10.5. Then, 500 mg of the microgels were added to the solution and kept at 50 $^{\circ}$ C for 24 h. The products were repeatedly washed with distilled water until neutral, and centrifuged with ethanol to obtain a white paste.³⁶

Preparation of microgels@aminoacids@crosslinked layer-coated chip. First, a pre-polymer solution consisting of 30 mg of microgels@amino acids, 50 μ L of NVP, 5 μ L of EGDMA, and 3 mg of DMPA were prepared in 50 μ L of DMSO. Then, 25 μ L of the pre-polymerization solution were placed on a quartz plate (10×10 cm). The QCM chip was placed faced down on the pre-polymerization solution and pressed with appropriate force (achieved by Lab-built pressure film machine). The chip was exposed to UV light (365 nm) for 1 h. The QCM chip was placed in distilled water and the polymer-coated chip was automatically detached from the quartz plate. Finally, the polymer-coated chip was rinsed with redistilled water repeatedly. Meanwhile, the microgels@crosslinked layer-coated chip was synthesized in the same way as the microgels@aminoacids@crosslinked layer-coated chip. And the formula is the same, with only microgels substituted for microgels@amino acids. 30 mg microgels were added to 100 μ L of ethanol and mixed evenly, 25 μ L of the solution was placed on the chip and then spin-coated with a homogenizer (3000 r/min). Distilled water was repeatedly washed to obtain the microgels-coated chip.

QCM measurements. The polymer coated-chip was dried with nitrogen and placed in the flow cell of the QCM. PBS (0.1 mol/L) was pumped into the flow cell continuously by using a peristaltic pump, and the frequency of the chip was monitored in real time using the QCM data acquisition software. After the frequency shift (ΔF) was stabilized, the glucose detection capacity and anti-pollution performance were evaluated.

Conflicts of interest

There are no conflicts to declare.

Acknowledgements

This work is supported by Science and Technology Service Network Project (STS Program) of Chinese Academy of Sciences (KJF-STS-ZDTP-063), the National Key Research and

Development Program of China (2016YFA0201600), the Ministry of Science and Technology focused on the research of "early identification, early diagnosis and cutting point of diabetes risk factors" (2016YFC1305700), the National Natural Science Foundation of China (Grant No. 51925203), Jiangsu Provincial Basic Public Health Service Innovation Pilot Project (WDF15-967), Jiangsu Medical Device Industry Technology Innovation Center Joint Fund (SYC2018004).

Notes and references

1. L. Lipani, B. G. R. Dupont, F. Doungmene, F. Marken, R. M. Tyrrell, R. H. Guy and A. Ilie, *Nat Nanotechnol.*, 2018, **13**, 504–511.
2. M. A. Pleitez, T. Lieblein, A. Bauer, Hertzberg, H. V. Lilienfeld-Toal and W. Mäntele, *Anal. Chem.*, 2013, **85**, 1013–1020.
3. Y. H. Chen, S. Y. Lu, S. S. Zhang, Y. Li, Z. Qu, Y. Chen, B. W. Lu, X. Y. Wang, X. Feng, *Sci Adv.*, 2017, **3**, e1701629.
4. J. E. Fradkin, C. C. Cowie, M. C. Hanlon and G. P. Rodgers, *Diabetes*, 2013, **62**, 3963–3967.
5. D. C. Klonoff, D. Ahn, A. Drincic, *Diabetes Res Clin Pr.*, 2017, **48**, 178–192.
6. E. Toschi, C. Slyne, A. Atakov-Castillo, J. Greenberg, T. Greaves, S. P. Carl and M. Munshi, *Diabetes*, 2018, **67**(Supplement 1).
7. S. F. Clarke and J. R. Foster, *Brit J Biomed Sci.*, 2012, **69**, 83–89.
8. S. Delbeck, T. Vahlsing, S. Leonhardt, G. Steiner and H. M. Heise, *Anal Bioanal Chem.*, 2019, **411**, 63–77.
9. J. Kim, A. S. Campbell, J. Wang, *Talanta*, 2018, **177**, 163–170.
10. K. Ngamchuea, C. Batchelor-McAuley and R. G. Compton, *Sensor Actuat B-Chem.*, 2018, **262**, 404–410.
11. J. T. L. Belle, A. Adams, C. E. Lin, E. Engelschall, B. Pratta and C. B. Cook, *Chem. Commun.*, 2016, **52**, 9197–9204.
12. R. P. Agrawal, N. Sharma, M. S. Rathore, V. B. Gupta, S. Jain, V. Agarwal and S. Goyal, *J Diabetes Metab.*, 2013, **4**, 1000266.
13. A. Soni and S. K. Jha, *Anal Chim Acta*, 2017, **996**, 54–63.
14. T. Arakawa, Y. Kurokia, H. Nitta, P. Chouhan, K. Tomaa, S. Sawada, S. Takeuchi, T. Sekita, K. Akiyoshi, S. Minakuchi, K. Mitsubayashi, *Biosens. Bioelectron.*, 2016, **84**, 106–111.
15. M. Gianneli, E. Polo, H. Lopez, V. Castagnola, T. Aastrup and K. A. Dawson, *Nanoscale*, 2018, **10**, 5474–5481.
16. M. Gianneli, E. Polo, H. Lopez, V. Castagnola, T. Aastrup and K. A. Dawson, *Nanoscale*, 2018, **10**, 5474–5481.
17. A. Webster, F. Vollmer and Y. Sato, *Nat Commun.*, 2014, **5**, 5284.
18. MonirehBakhshpour, AyseKevser, Piskin, Handan Yavuz, AdilDenizli, *Talanta*, 2019, **204**, 840–845.
19. D. Meléndrez, T. Jowitt, M. Iliut, A. F. Verre, S. Goodwin and A. Vijayaraghavan, *Nanoscale*, 2018, **10**, 2555–2567.
20. E. S. Parsons, G. J. Stanley, A. L. B. Pyne, A. W. Hodel, A. P. Nievergelt, A. Menny, A. R. Yon, A. Rowley, R. P. Richter, G. E. Fantner, D. Bubeck and B. W. Hoogenboom, *Nat Commun.*, 2019, **10**, 2066.
21. H. T. Yang, P. Li, D. Z. Wang, Y. Liu, W. Wei, Y. J. Zhang and S. Q. Liu, *Anal. Chem.*, 2019, **91**, 17, 11038–11044.
22. M. A. Aboudzadeh, M. Sanromán-Iglesias, C. H. Lawrie, M. Grzelczak, L. M. Liz-Marzán and T. Schäfer, *Nanoscale*, 2017, **9**, 16205–16213.
23. Z. M. Marsh, K. A. Lantz and M. Stefk, *Nanoscale*, 2018, **10**, 19107–19116.
24. R. H. Wang, L. J. Wang, Z. T. Callaway, H. G. Lu, T. J. Huang and Y. B. Li, *Sensors and Actuators B*, 2017, **240**, 934–940.
25. P. Zhang, L. Q. Kong, H. H. Wang and D. Z. Shen, *Sensors and Actuators B*, 2017, **238**, 44–753.
26. K. Ngamchuea, K. Chaisiwamongkhon, C. Batchelor-McAuley and R. G. Compton, *Analyst*, 2018, **143**, 81–99.
27. S. Al Kawas, Z. H. A. Rahim and D. B. Ferguson, *Arch Oral Biol.*, 2012, **57**, 1–9.
28. Y. Uludag and I. E. Tothill, *Anal. Chem.*, 2012, **84**, 5898–5904.
29. H. Y. Wu, C. J. Lee, H. F. Wang, Y. Hu, M. Young, Y. Han, F. J. Xu, H. B. Cong and G. Cheng, *Chem. Sci.*, 2018, **9**, 2540–2546.
30. Y. Nagasaki, H. Kobayashi, Y. Katsuyama, T. Jomura and T. Sakura, *J Colloid Interf Sci.*, 2007, **309**, 524–530.
31. Y. C. Hu, B. Liang, L. Fang, G. G. Ma, G. Yang, Q. Zhu, S. F. Chen and X. S. Ye, *Langmuir*, 2016, **32**, 11763–11770.
32. R. Mo, T. Y. Jiang, J. Di, W. Y. Tai and Z. Gu, *Chem. Soc. Rev.*, 2014, **43**, 3595–3629.
33. Y. Guan, Y. Zhang, *Soft Matter*, 2011, **7**, 6375–6384.
34. J. B. Thorne, G. J. Vine and M. J. Snowden, *Colloid Polym Sci.*, 2011, **289**, 625–646.
35. F. Wang, Y. T. Zhang, P. Yang, S. Jin, M. Yu, J. Guo and C. C. Wang, *J. Mater. Chem. B*, 2014, **2**, 2575–2582.
36. C. Xu, X. Hu, J. Wang, Y. M. Zhang, X. J. Liu, B. B. Xie, C. Yao, Y. Li and X. S. Li, *ACS Appl. Mater. Interfaces.*, 2015, **7**, 17337–17345.
37. S. Chen, S. Jiang, *Adv. Mater.*, 2008, **20**, 335–338.
38. A. M. Alswieleh, N. Cheng, I. Canton, B. Ustbas, X. Xue, V. Ladmiral, S. J. Xia, R. E. Ducker, O. E. Zubir, M. L. Cartron, C. N. Hunter, G. J. Leggett and S. P. Armes, *J. Am. Chem. Soc.*, 2014, **136**, 9404–9413.
39. Q. Li, J. Imbrogno, G. Belfort, X. L. Wang, *J Appl Polym Sci.*, 2015, **132**, 41781.
40. Y. N. Chou, Y. Chang and T. C. Wen, *ACS Appl. Mater. Interfaces.*, 2015, **7**, 10096–10107.
41. Z. X. Zhang, Q. Dou, H. K. Gao, B. Bai, Y. M. Zhang, D. B. Hu, A. K. Yetisen, H. Butt, X. X. Yang, C. J. Li and Q. Dai, *Adv. Healthcare Mater.*, 2018, **7**, 1700873.
42. Q. C. Cao, X. Wang and D. C. Wu, *Chinese J. Polym. Sci.*, 2018, **36**(1), 8–17.
43. H. S. Guo, Y. Jing, W. Q. Zhao, T. Xua, C. G. Line, J. W. Zhang and L. Zhang, *Chemical Engineering Journal*, 2019, **374**, 1353–1363.
44. Q. Li, Q. Y. Bi, H. H. Lin, L. X. Bian and X. L. Wang, *Journal of Membrane Science*, 2013, **427**, 155–167.
45. R. J. Ma and L. Q. Shi, *Polym. Chem.*, 2014, **5**, 1503–1518.
46. D. Shen, H. J. Yu, L. Wang, A. Khan, F. Haq, X. Chen, Q. Huang and L. S. Teng, *Journal of Controlled Release*, 2020, **321**, 236–258.
47. A. M. Horgan, A. J. Marshall, S. J. Kew, K. E. S. Dean, C. D. Creasey, S. Kabilan, *Biosens Bioelectron.*, 2006, **21**, 1838–1845.
48. J. Q. Wang, Z. J. Wang, J. C. Yu, A. R. Kahkoska, J. B. Buse and Z. Gu, *Adv. Mater.*, 2019, 1902004.
49. S. Chiappin, G. Antonelli, R. Gatti and E. F. De Palo, *Clin Chim Acta.*, 2007, **383**, 30–40.
50. K. Ngamchuea, K. Chaisiwamongkhon, C. Batchelor-McAuley and R. G. Compton, *Analyst*, 2018, **143**, 81–99.
51. M. Lazerges, H. Perrot, N. Rabehagaso and C. Compère, *Biosensors*, 2012, **2**, 245–254.
52. P. Vejayakumaran, I. A. Rahman, C. S. Sipaut, J. Ismail and C. K. Chee, *J Colloid Interf Sci.*, 2008, **328**, 81–91. «地址块»